Journal of Modern Optics
Vol. 52, No. 9, 15 June 2005, 1197–1206

Taylor & Francis
Taylor & Francis Group

Compensation of third-order dispersion in a 100 Gb/s single channel system with in-line fibre Bragg gratings

E. J. GUALDA, L. C. GÓMEZ-PAVÓN and J. P. TORRES*

ICFO-Institut de Ciències Fotòniques and Department of Signal Theory and Communications, Polytechnic University of Catalonia, 08034 Barcelona, Spain

(*Received 30 June 2004; in final form 7 October 2004*)

This paper presents a scheme to enhance the performance of an ultrahigh capacity (100 Gb/s) long haul transmission system that makes use of chirped fibre Bragg gratings (FBG) for dispersion slope compensation. It is shown that the FBG effectively compensate the dispersion slope while at the same time providing appropriate in-line filtering. The penalty to the system performance due to unwanted group delay ripple is also discussed.

1. Introduction

Wavelength division multiplexing (WDM) allows the design of optical transmission systems with aggregate capacities exceeding 1 Tbit/s over transoceanic distances [1]. The use of higher bit rates for single channel propagation is of interest in dense WDM systems, since the same total capacity of the link can be achieved with a reduction of the total bandwidth used. Moreover, single channel ultrahigh capacities in shorter distances (~1000 km) are of interest for some specific applications.

As pointed out in [2], dispersion slope is particularly troublesome when increasing the bit rate of the system. The dispersion length associated with third order dispersion length scales as $\sim T^3$, where $B = T^{-1}$ is the bit rate of the system. Thus, an increase from 10 Gb/s to 100 Gb/s reduces the dispersion length by a factor of 100.

Since chirped fibre Bragg gratings (FBG) were first proposed as dispersion compensators [3], optical fibre links with longer lengths and higher capacity that make use of chirped FBG for dispersion compensation have been demonstrated [4, 5]. FBGs are an effective solution for dispersion compensation, especially because of the absence of nonlinear effects. Chirped FBG can also be used to compensate third-order dispersion [6–9], as well as more complex dispersion compensation profiles with very low values of group delay ripple (GDR) [10].

Here, we consider a scheme for dispersion slope compensation of ultrahigh capacity (100 Gb/s) long haul single channel systems that make use of in-line chirped FBGs for dispersion slope compensation. Chirped FBGs for pure dispersion slope compensation are of interest here, since the second-order chromatic dispersion will

*Corresponding author. Email: jperez@tsc.upc.edu

Journal of Modern Optics
ISSN 0950–0340 print/ISSN 1362–3044 online
http://www.tandf.co.uk/journals
DOI: 10.1080/09500340512331327543

be compensated with an appropriately designed dispersion map. An ultrahigh bit rate (100 Gb/s) system that makes use of FBG to compensate dispersion has been demonstrated in a 77 km long optical fibre system [11]. On the other hand, a 16×10 Gb/s system with in-line gratings for dispersion compensation has also been demonstrated [4]. When going to higher single channel bit rates and higher distances, as considered in this paper, one should make use of carefully designed dispersion compensation schemes in order to avoid unacceptable degradation of the eye opening. We propose a new dispersion compensation scheme that makes use of a combination of properly designed dispersion maps for second-order dispersion compensation, and a properly designed FBG to compensate for dispersion slope; it allows the design of optical fibre systems with very high single-channel capacity over long distances. We also consider the limitations imposed on the performance of the system due to the presence of unwanted group delay ripple (GDR), due to systematic and random errors produced in the chirped FBG during the fabrication process. In long distance (>1000 km) optical fibre systems, GDR can severely degrade system performance, so that it is of great interest to determine the amount of GDR that can be tolerated in the fabrication process of a FBG. Recently, several techniques have been developed to reduce the amount of GDR, reducing significantly the penalty imposed on system performance [12–14].

2. Description of the system

Here we consider the 100 Gb/s single channel ($\lambda = 1.55\,\mu$m) system discussed in [2]. The modulation format is return-to-zero (RZ), where the RZ pulses have a raised cosine shape, i.e. $u(t) = \sqrt{P_0/4}[1 + \cos(2\pi t/T)]$, where t is time, P_0 is peak power and $T = 10$ ps, which corresponds to a bit rate $B = 100$ Gb/s. The dispersion map is designed to minimize the deleterious effects of chromatic dispersion and nonlinearities in the fibre. It makes use of two types of fibre: spans with normal dispersion ($D = -0.3$ ps/nm/km at 1550 nm) and spans with anomalous dispersion ($D = 0.3$ ps/nm/km at 1550 nm). Each section of the system is composed of 10 km of fibre with anomalous dispersion, sandwiched between two spans of 5 km with normal dispersion. The attenuation is $\alpha = 0.2$ dB/km. The evolution of the light pulses in each section is described by two coupled nonlinear Schrödinger equations [15, 16]:

$$\begin{aligned} & i\frac{\partial A_x}{\partial z} - \beta_1 \frac{\partial^2 A_x}{\partial t^2} - \frac{1}{2}\beta_2 \frac{\partial^2 A_x}{\partial t^2} - \frac{i}{6}\beta_3 \frac{\partial^3 A_x}{\partial t^3} \\ & \quad + \gamma\left(|A_x|^2 + \frac{2}{3}|A_y|^2\right)A_x + i\alpha A_x = 0 \\ & i\frac{\partial A_y}{\partial z} + \beta_1 \frac{\partial^2 A_y}{\partial t^2} - \frac{1}{2}\beta_2 \frac{\partial^2 A_y}{\partial t^2} - \frac{i}{6}\beta_3 \frac{\partial^3 A_y}{\partial t^3} \\ & \quad + \gamma\left(|A_y|^2 + \frac{2}{3}|A_x|^2\right)A_y + i\alpha A_y = 0 \end{aligned} \tag{1}$$

where A_x and A_y are the slow varying amplitudes of the field along the x and y axes, associated to each linear polarization respectively; β_1 is the inverse group velocity, β_2 is the group velocity dispersion, which is related to the second-order dispersion

parameter D by $\beta_2 = -\lambda^2 D/(2\pi c)$, β_3 is the third order dispersion parameter, which is related to the slope dispersion parameter S by $\beta_3 = -\lambda^4 S\ /(2\pi c)^2$. The dependence of the dispersion of the fibre as a function of the wavelength is given by $D = S{\cdot}(\lambda - \lambda_0) + D(\lambda_0)$. We consider a value of the dispersion slope parameter of $S = 0.1\ \text{ps/nm}^2\text{/km}$, which for the modulation format considered here and a peak power of $P_0 = 1\ \text{mW}$, clearly produces an eye diagram that is not acceptable [2]. The nonlinear coefficient is $\gamma = \omega \cdot n_2/A_{\text{eff}}\, c$. The nonlinear Kerr coefficient $n_2 = 2.6 \times 10^{-20}\ \text{m}^2\text{/W}$ is the same for both types of fibres and the effective area of the fibres is $A_{\text{eff}} = 55\ \mu\text{m}^2$. In order to take into account the penalty to the system performance of polarization mode dispersion (PMD), we assume that the fast and slow axis randomly rotates along the fibre at intervals z_{h}, while at the same time a random phase factor between both polarizations is added [17]. The PMD parameter is given by [18] $D_{\text{p}} = \sqrt{8/3\pi}(\Delta n/c)\sqrt{z_{\text{h}}}$, where c is the light velocity, the polarization beat length is $L_{\text{B}} = 33\ \text{m}$ and the fibre correlation length is $z_{\text{h}} = 100\ \text{m}$.

At the end of each section, the optical signal is amplified and filtered, with optical in-line fourth-order Bessel filters with 1200 GHz bandwidth (FWHM, full width half maximum), since in-line filtering can enhance the performance of the system [19]. When the filter response function is expanded in a Taylor series, one can substitute equation (1) by a simplified propagation equation that takes into account the effect of in-line filtering [20]. Notwithstanding, in this paper we always consider the full response of the filters. The excess noise factor of the amplifiers is $n_{\text{sp}} = 1.5$. On the receiver end, the signal field is detected by means of a photodiode, mathematically described by a square law device, followed by electrical low-pass filtering with a fifth-order Bessel filter with 85 GHz bandwidth (FWHM).

To solve equation (1), we make use of a standard FFT split-step method. An appropriate amount of Gaussian noise is added to each component of the Fourier spectrum of the optical signal at each amplifier [21] to simulate the effect of spontaneous emission of the EDFA.

In figure 1(*a*) we show the eye diagram of the received signal after propagating 2000 km when the dispersion slope is negligible ($S = 0$). Figure 1(*b*) shows the eye diagram for $S = 0.1\ \text{ps/nm}^2\text{/km}$. One observes that for this value of the dispersion slope parameter, the performance of the system highly degrades. Thus a dispersion slope compensation scheme is required to enhance the performance of the optical system.

In order to compensate for the detrimental effect on system performance of dispersion slope compensation, we consider the introduction of in-line FBG for dispersion slope compensation. The refractive index of a FBG presents a modulation that can be written as [22] $n(z) = n_0 + \triangle n_{\text{g}}(z)\cos(2K_0 z + \theta(z))$ where n_0 is the average effective refractive index of the grating core, $\triangle n_{\text{g}}$ is the local grating strength (apodization), $K_0 = \pi/\Lambda$ is the wave number at the design wavelength, Λ is the nominal period of the refractive index change and $\theta(z) = C_2/6 \cdot z^3 + C_1/2 \cdot z^2$ describes the grating chirp. The properties of the FBG can be obtained with the help of coupled mode theory [22, 23], where one obtains two equations for the forward propagating wave U and the backward propagating wave V:

$$\begin{aligned} \frac{\partial U(z)}{\partial z} &= -i\Delta U(z) - i\kappa(z)V(z) \\ \frac{\partial V(z)}{\partial z} &= i\Delta V(z) + i\kappa^*(z)U(z) \end{aligned} \tag{2}$$

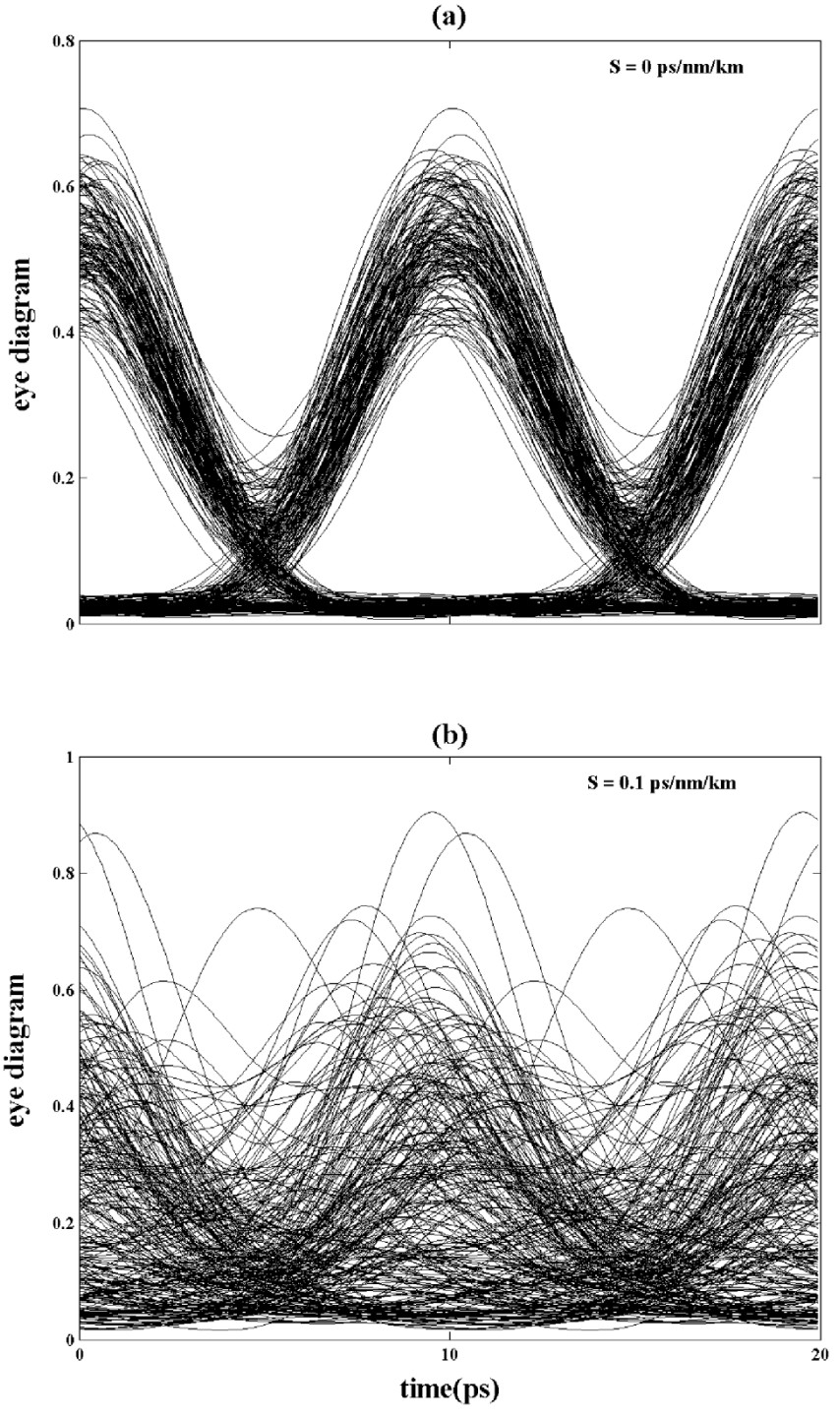

Figure 1. Eye diagram of the electrical signal after propagating 2000 km. In (*a*) the dispersion slope is considered negligible ($S = 0\,\mathrm{ps/nm^2/km}$) and in (*b*) the dispersion slope coefficient is $S = 0.1\,\mathrm{ps/nm^2/km}$. In both cases, five realizations with 64 bits each are represented. The PMD parameter is $D_\mathrm{p} = 0.05\,\mathrm{ps/km^{1/2}}$.

where $\Delta = (\omega - \omega_0)/\omega_0$ is the normalized detuning, $\omega_0 = 2\pi c/\lambda_0$ is the central frequency, ω is the frequency and the coupling coefficient κ is given by $\kappa(z) = \kappa_0 \cdot f(z)$. The constant $\kappa_0 = \pi \cdot \delta n/2\lambda_0 n_0$ is the maximum coupling coefficient, δn is the refractive index change, n_0 is the mean refractive index of the grating and $f(z)$ is an hyperbolic tangent apodization profile [22, 23], which is characterized by a measure of the sharpness of the grating edges (a) and the length of the grating (L). This function has been shown to give better performance than other apodization functions. In all cases, we will consider the full spectral response of the FBG.

For a spacing of the FBG of 200 km, they should compensate a dispersion slope given by the product $S \cdot L = 20\,\text{ps/nm}^2$ and not to introduce any extra dispersion compensation. This can be achieved by using a combination of two chirped FBG with opposite chirps [7]. If we fix the parameters $C_1 = 10\,\text{cm}^{-2}$ and $C_2 = 0.015\,\text{cm}^{-3}$, one can achieve the required dispersion slope compensation for a grating with a length $L = 32\,\text{cm}$ over a bandwidth of $\sim$2.8nm. Figures 2(a) and 2(b) show the spectral response of one individual grating and of the combination of the two gratings with opposite values of the chirp profile, respectively. While the dispersion compensation of both FBG cancelled, each one compensates exactly half of the total amount of dispersion slope.

In figure 3 we plot the eye diagram when dispersion slope compensation provided by the chirped FBG is considered. For the sake of comparison, figure 3(a) shows the back-to-back eye diagram, when only the noise of the amplifiers is considered. Figure 3(b) shows that the FBG effectively enhance the performance of the system by compensating the dispersion slope introduced by the propagation. Since the FBG also behaves as filters, the presence of the FBG can replace the necessity of additional in-line filtering. The FBG gratings used have a bandwidth of 2.8 nm and are spaced 200 km, while the Bessel optical filters have a bandwidth of nearly 10 nm and are spaced 20 km apart. Moreover, the FBG has a flatter response near the central wavelength.

3. Effect of group delay ripple

Group delay ripple can severely degrade the performance of the system [24]. This drawback is more severe when, as is the case considered here, several FBG are concatenated. In order to evaluate the influence of grating imperfections on the system performance, we add sinusoidal variations in the group delay profile of the chirped FBG slope compensator. The GDR added to the group delay profile is defined by [25] $\Delta\tau_{\text{GSR}} = A_{\text{GDR}}/2 \cdot \cos(\omega T_{\text{GDR}} + \theta_{\text{GDR}})$ where $1/T_{\text{GDR}}$ is the period of the perturbation and A_{GDR} is the peak-to-peak amplitude of the ripples. To take into account the random behaviour of the GDR profile, the relative phase of the GDR pattern of each pair of gratings, θ_{GDR}, is considered to be uniformly distributed between 0 and 2π.

We calculate the EOP for different periods and amplitudes of the ripples. The EOP is defined as the ratio between the eye opening at the link output and the eye opening of the back-to-back system [26]. In figure 4(a) we plot the EOP as a function of the systems length for the case with $A_{\text{GDR}} = 1$ ps and different periods of the GDR.

Figure 4(b) shows the better and the worst EOP obtained from simulations for gratings with ripple $1/T_{\text{GDR}} = 200\,\text{GHz}$ and $A_{\text{GD}R} = 1\,\text{ps}$, at a distance of

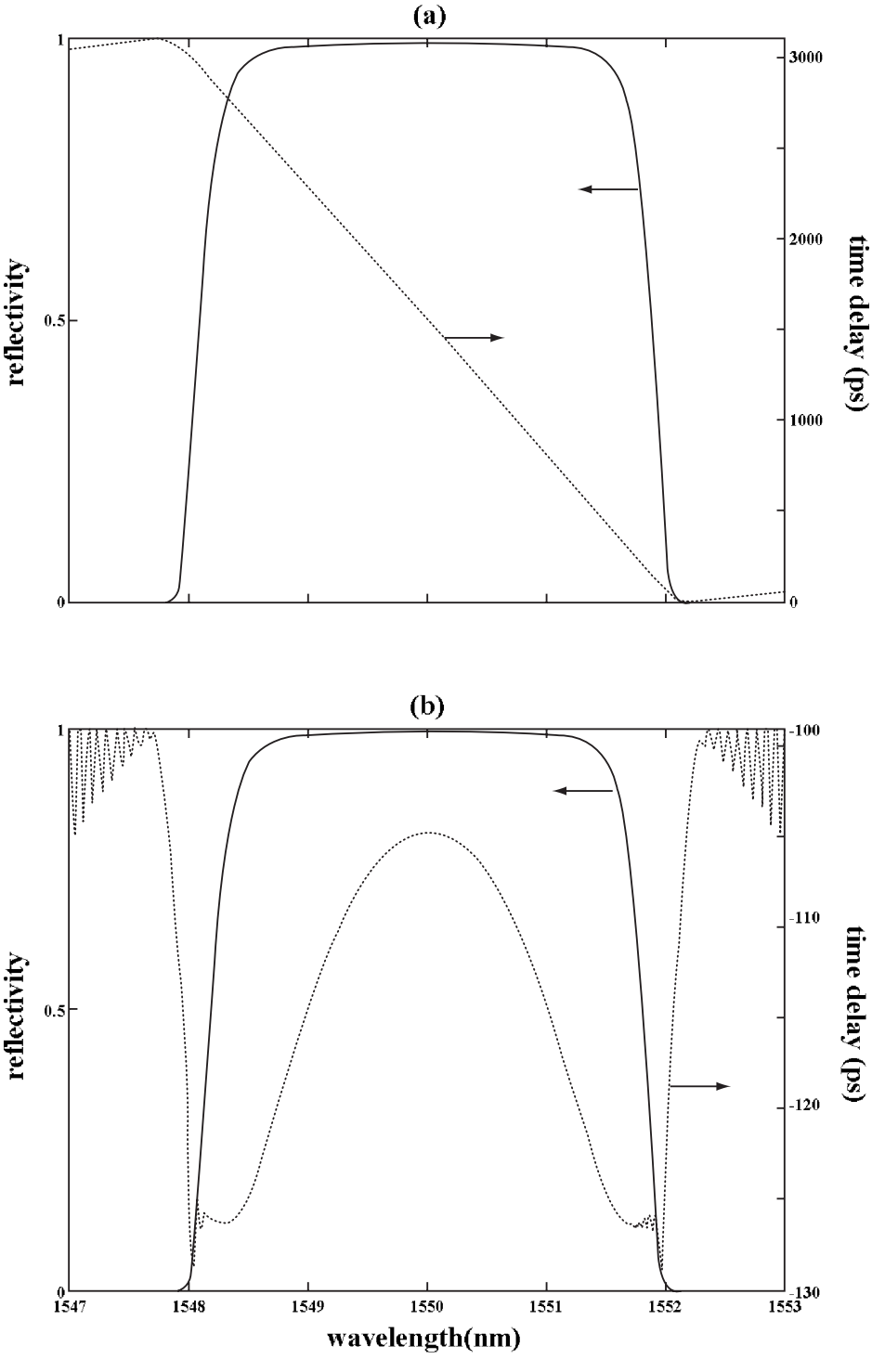

Figure 2. Reflectivity and group delay of the FBG used for dispersion compensation slope with measure of the sharpness $a = 4$. (*a*) Response of each individual grating and (*b*) response of two combined FBG with opposite chirp.

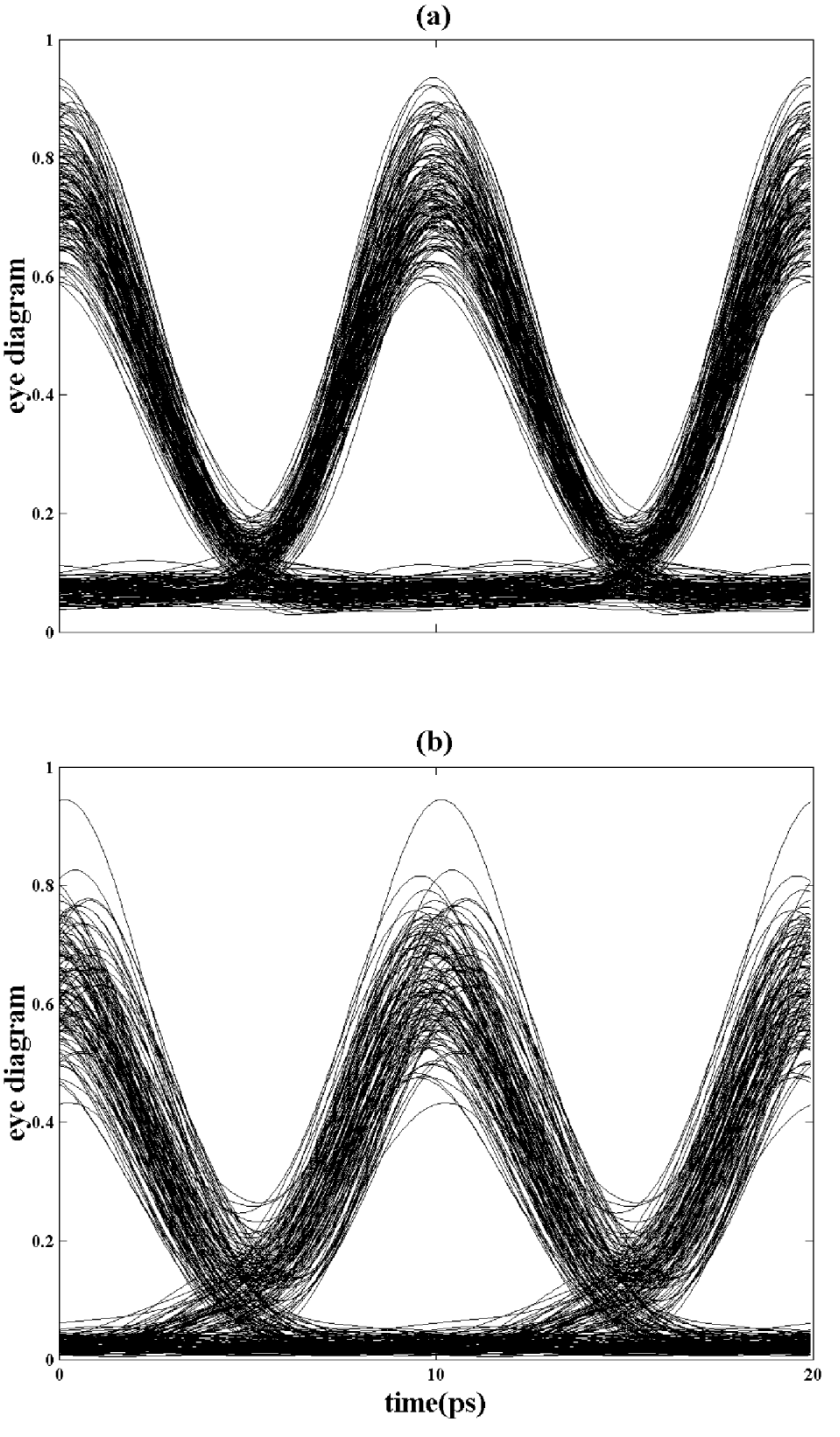

Figure 3. Eye diagram of the electrical signal at the receiver. In (*a*) we show the back-to-back eye diagram (only noise is considered) and in (*b*) when the FBG are used as dispersion slope compensators; the Bessel in-line filters are removed. In both cases, five realizations with 64 bits each are represented. The PMD parameter is $D_p = 0.05\,\mathrm{ps/km^{1/2}}$.

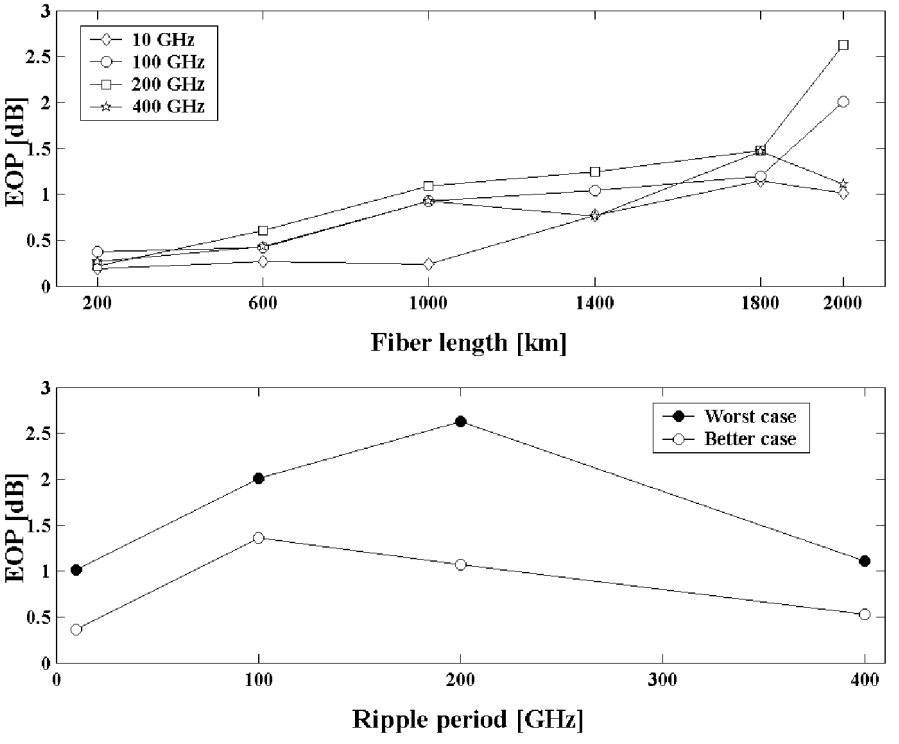

Figure 4. Worst eye opening penalty in dB for different periods of the ripple with $A_{GDR} = 1$ ps at different fibre length. In the lower picture, better and worst cases are represented for 2000 km. Five simulations for each period are considered. The solid line is to help the eye.

$L = 2000$ km. We observe that the EOP is worst for periods comparable with the bit rate of system [27]. For short periods the effect of GDR averages out, leading to only a minor impact on the signal, whereas for long periods the GDR acts as a perturbation of the nominal value of the slope compensation. Figure 5 shows the worst eye diagram obtained for $L = 1000$ km and $L = 2000$ km. The EOP penalty for the system with $L = 1000$ km is around 1 dB.

4. Conclusions

We have shown that an in-line chirped FBG for dispersion slope compensation can enhance the performance of ultrahigh capacity single channel optical transmission systems when system performance degradation is a result of the dispersion slope introduced in the propagation. Moreover, we have considered the penalty introduced in the system performance due to GDR. It has been shown that the maximum length of the system is severely limited by group delay ripple of the gratings, which would require further improvements in group delay correction systems, which is currently an active line of research [13, 14]. FBG with a 1 ps peak-to-peak GDR

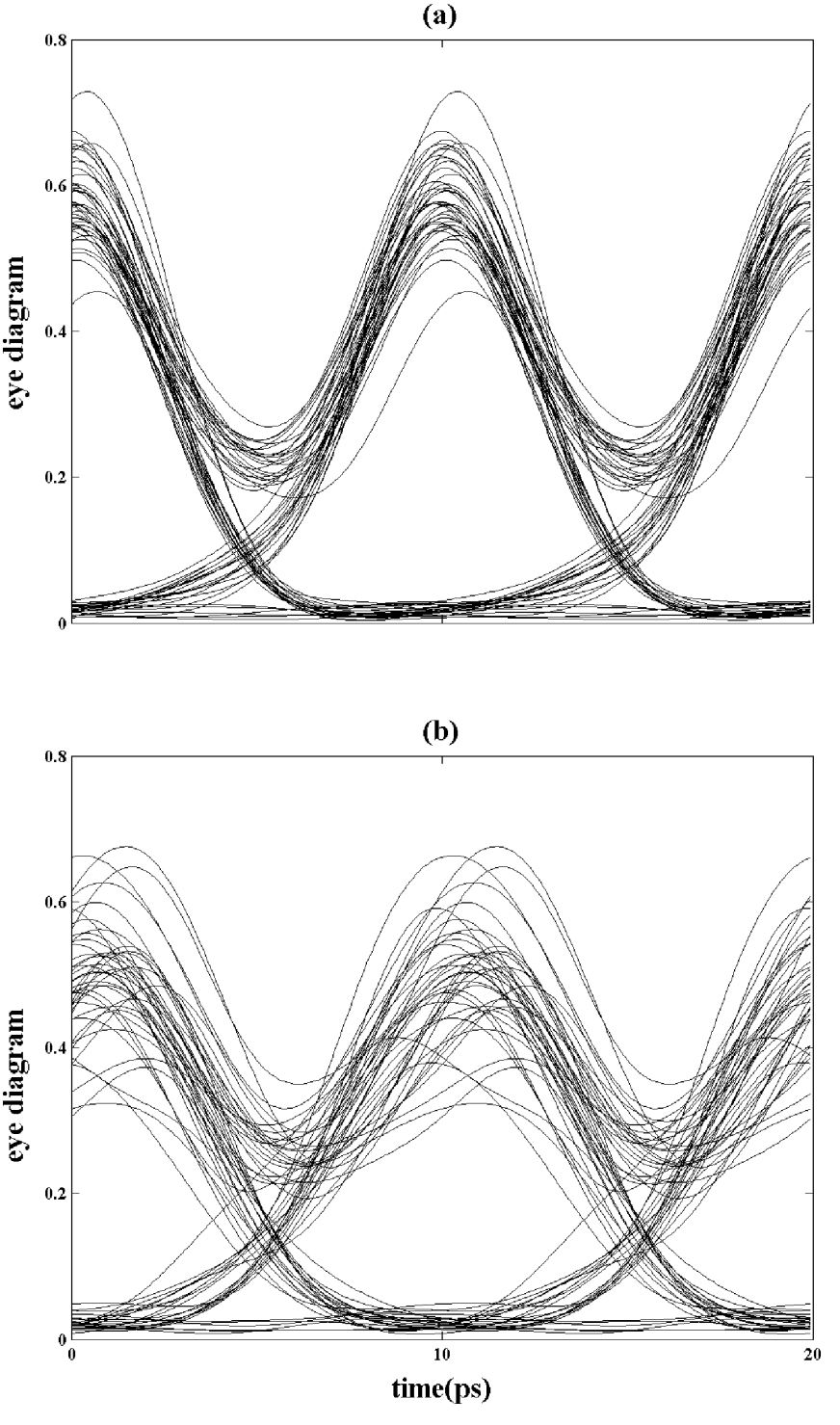

Figure 5. Worst eye diagrams of the electrical signal with slope compensation module with ripple $A_{\mathrm{GDR}} = 1\,\mathrm{ps}$ and $1/T_{\mathrm{GDR}} = 200\,\mathrm{GHz}$: (*a*) after propagating 1000 km (*b*) after propagating 2000 km.

amplitude, can introduce a penalty of less than 1 dB in systems with a distance shorter than 1000 km.

References

[1] J.X. Cai, M. Nissov, C.R. Davidson, *et al*., IEEE J. Lightw. Technol. **20** 2247 (2002).
[2] D. Marcuse and C.R. Menyuk, Opt. Lett. **17** 564 (1999).
[3] F. Oulette, Opt. Lett. **12** 847 (1987).
[4] L.D. Garret, A.H. Gnauck, F. Forghieri, *et al*., IEEE Photonics Technol. Lett. **11** 484 (1999).
[5] A. Sahara, T. Komukai, E. Yamada, *et al*., Electron. Lett. **37** 8 (2001).
[6] J.A.R. Williams, L.A. Everall, I. Bennion, *et al*., IEEE Photonics Technol. Lett. **8** 1187 (1996).
[7] T. Komukai and M. Nakazawa, Opt. Commun. **154** 5 (1998).
[8] C.S. Goh, S.Y. Set, K. Taira, *et al*., IEEE Photonics Technol. Lett. **14** 663 (2002).
[9] M. Ibsen and M. Feced, *Tech. Dig. Conf. Opt. Fibre Commun. paper FA7.2002* (2002).
[10] Y. Liu, L. Dong, J.J. Pan, *et al*., Opt. Lett. **28** 786 (2003).
[11] M.J. Guy, J.R. Taylor and R. Kashyap, Opt. Commun. **150** 77 (1998).
[12] T. Komukai, T. Inui and M. Nakazawa, IEEE Photonics Technol. Lett. **12** 816 (2000).
[13] A.V. Buryak and D.Y. Stepanov, Opt. Lett. **27** 1099 (2002).
[14] M. Sumetsky, P.I. Reyes, P.S. Westbrook, *et al*., Opt. Lett. **28** 777 (2003).
[15] C.R. Menyuk, IEEE J. Quantum Electron. **25** 2674 (1989).
[16] F. Matera, M. Settembre, M. Tamburrini, *et al*., J. Lightw. Technol. **17** 2225 (1999).
[17] P.K.A. Wai, C.R. Menyuk and H.H. Chen, Opt. Lett. **16** 1231 (1991).
[18] M. Matsumoto, Y. Akagi and A. Hasegawa, IEEE J. Lightw. Technol. **15** 584 (1997).
[19] E.A. Golovchenko, J.M. Jacob, A.N. Pilipetski, *et al*., Opt. Lett. **22** 289 (1997).
[20] L. Mollenauer, J.P. Gordon, S.G. Evangelides, *et al*., Opt. Lett. **17** 1575 (1992).
[21] D. Marcuse, Opt. Lett. **17** 34 (1992).
[22] T. Erdogan, IEEE J. Lightw. Technol. **15** 1277 (1994).
[23] K. Ennser, M.N. Zervas and R.I. Laming, IEEE J. Quantum Electron. **34** 770 (1998).
[24] S.G. Evangelides, N.S. Bergano, C.R. Davidson, *Optical Fibre Conference*, February, *paper FA2.1999* (1999).
[25] Y.H.C. Kwan, P.K.A. Wai and H.Y. Tam, Opt. Lett. **26** 959 (2001).
[26] F. Matera and M. Settembre, J. Sel. Top. Quantum. Electron. **6** 308 (2000).
[27] K. Ennser, M. Ibsen, M.N. Zervas, *et al*., IEEE Photonics Technol. Lett. **10** 1476 (1998).